

Supporting information

Circularly Polarized Luminescence and Performance Modulation of Chiral Europium-Titanium-Oxo Clusters Eu₂Ti₄

Wei-Dong Liu¹, Guan-Jun Li¹, Han Xu¹, Yong-kai Deng^{1,2}, Ming-Hao Du¹, La-Sheng Long¹, Lan-Sun Zheng¹ and Xiang-Jian Kong^{1*}

¹ Collaborative Innovation Center of Chemistry for Energy Materials, State Key Laboratory of Physical Chemistry of Solid Surfaces, and Department of Chemistry, College of Chemistry and Chemical Engineering, Xiamen University, Xiamen 361005, P. R. China.

² School of Chemistry and Chemical Engineering, State Key Laboratory of Crystal Materials, Shandong University, Jinan 250100, P. R. China.

*Corresponding author: *xjkong@xmu.edu.cn*

Content

Physical Measurements	2
Synthesis and characteristics of 4,5-pinene-2,2'-bipyridine enantiomers.....	4
Synthesis of (+)-4,5-Pinene-2,2'-Bipyridine.....	4
Synthesis of (-)-4,5-Pinene-2,2'-Bipyridine.....	7
Synthesis and characteristics of chiral europium-titanium-oxo clusters.....	10
Synthesis of 1-6	10
Single crystal structure refinements of 1-6	12
Detailed bond distances and bond angles of 1-6	22

Physical Measurements

X-ray Crystallography

The crystal data of 4,5-pinene-2,2'-bipyridine enantiomers and **1-6** were collected on a Rigaku Oxford Diffraction XtaLAB Synergy diffractometer with micro-focus sealed X-ray Cu K α radiation ($\lambda = 1.54184 \text{ \AA}$) at 100 K. Crystallography data reduction and faces absorption correction were performed using CrysAlisPro software (Rigaku Oxford Diffraction, 2015). The structure was solved by intrinsic phasing (SHEXT) and refined by full-matrix least-squares calculations based on F^2 using the SHELXTL-2018 software package. All the nonhydrogen atoms are refined anisotropically. The solvent contribution to the scattering factors of 4,5-pinene-2,2'-bipyridine enantiomers and **1-6** has been taken into account with PLATON/SQUEEZE. Detailed crystal data and structure refinement parameters for 4,5-pinene-2,2'-bipyridine enantiomers and **1-6** are listed in **Table S5** and **Table S7-S9** in the Supporting Information.

Luminescence and Circularly Polarized Luminescence (CPL) Measurements

The excitation and emission spectra of the room-temperature luminescence were measured on the steady-state and transient fluorescence spectrometer (FLS-1000, Edinburgh) equipped with a 450W Xenon lamp. The time-resolved PL decay curve was obtained on the same instrument with a microsecond flashlamp. The absolute quantum yield was collected also on the FLS-1000 at room temperature using a calibrated integrating sphere (coating with a PTFE-like material with a reflectance >99%) as the chamber. The circularly polarized luminescence spectra were measured on the circularly polarized luminescence pectrometer (CPL-200, JASCO). The $1 \times 10^{-5} \text{ M}$ CH_2Cl_2 solutions of **1-6** were prepared. The CPL measurements were performed at room temperature. The acquisition step is 1 nm and the acquisition time is one data point / 2 s.

Nuclear magnetic resonance (NMR)

^1H NMR spectra of 4,5-pinene-2,2'-bipyridine enantiomers were recorded at room temperature on a Avance III HD (500 MHz ^1H NMR, δ/ppm), the chemical shifts are reported in ppm. The solvent used was deuterated chloroform CDCl_3 .

High-resolution electrospray ionization mass spectrometry (HRESI-MS)

The high-resolution electrospray ionization mass spectrometry was performed on Agilent Technologies ESI-TOF-MS 6224A instrumentation. Typical measurement conditions are as follows: end plate offset = -400 V; dry gas = 3 L·min⁻¹, nebulizer = 0.3 bar, capillary voltage = 3500 V, sample flow rate = 4 L·min⁻¹. The data analysis of mass spectrum was performed based on the isotope distribution patterns using Compass Data Analysis software.

Circular Dichroism (CD)

Dispersing one crystal into 100 mg KBr by grinding could effectively reduce the macroscopic anisotropic arrangement, and the mixtures were tableted for testing. The circular dichroism (CD) spectra were recorded on a JASCO J-810 spectropolarimeter at room temperature.

UV-Vis spectroscopy

The UV-Vis absorption spectra of 4,5-pinene-2,2'-bipyridine enantiomers and CH₂Cl₂ solutions of **1-6**, and diffuse reflectance spectra (DRS) of **1-6** were obtained on a UV/Vis/NIR Spectrophotometer (PerkinElmer, Lambda 1050+).

Elemental Analysis

Microanalyses of C, H and O elements were carried out with an Element Analyzer (EA, Flash Smart CHNS/O).

Thermogravimetric Analysis (TGA)

Thermogravimetric analysis was prepared in N₂ using a Thermogravimetric analysis-Mass spectrometry (TGA-MS, SDT-650).

Fourier Transform Infrared Spectroscopy (FT-IR)

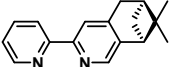
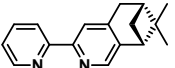
The infrared spectra were recorded on an In situ FT-IR Spectrometer (Bruker Vertex 70V) utilizing a single attenuated total reflectance (ATR) accessory.

Powder X-ray diffraction (PXRD)

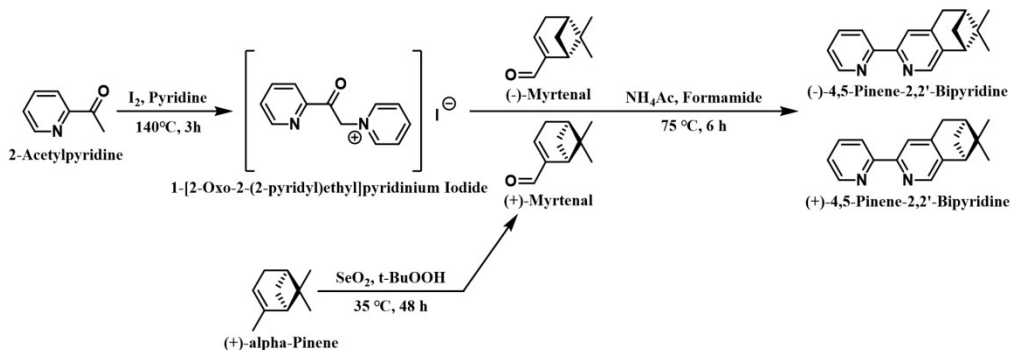
The powder X-ray diffraction (PXRD) pattern was recorded on the Rigaku Smartlab-SE diffractometer using Cu-K α radiation at 25 kV and 100 mA with a scanning rate of 5°/min.

Synthesis and characteristics of 4,5-pinene-2,2'-bipyridine enantiomers.

Table S1. The information on 4,5-pinene-2,2'-bipyridine enantiomers.

Chemical	CAS	Formula	MW	Chemical Structure
(+)-4,5-Pinene-2,2'-Bipyridine	177932-45-5	C ₁₇ H ₁₈ N ₂	250.34	
(-)-4,5-Pinene-2,2'-Bipyridine	144176-23-8	C ₁₇ H ₁₈ N ₂	250.34	

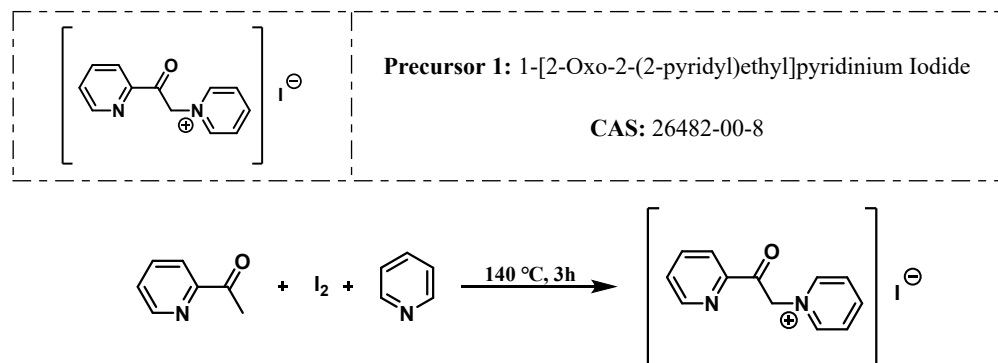
Synthesis Routes of the 4,5-pinene-2,2'-bipyridine enantiomers:



Synthesis of (+)-4,5-Pinene-2,2'-Bipyridine

The synthesis of (+)-4,5-pinene-2,2'-bipyridine requires the synthesis of two precursors first, requiring a total of three reactions.^[1]

Step 1: Synthesis of 1-[2-Oxo-2-(2-pyridyl)ethyl]pyridinium Iodide.



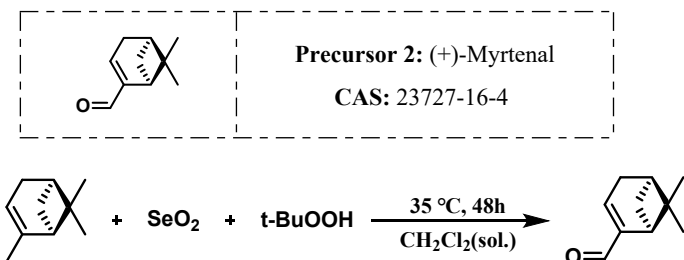
2-acetylpyridine (6.06 g, 50 mmol) and iodine (12.69 g, 50 mmol) were added to a 100 mL round-bottom flask. Then add 40 mL of pyridine and fully dissolve the solid. Heated to 140 °C and refluxed for 3 h. After the reaction, the round-bottom flask was cooled with an ice bath at 0 °C for 30 min. Suction-filtered the reaction mixture under reduced pressure. The solid product was washed several times with a small amount of icy pyridine and acetone and dried under vacuum to

obtain a gray-black solid without further purification (yield: 45.8%).

Table S2. The information on used chemicals in *step 1*.

Chemical	CAS	Formula	MW / FW	Purity Level	Brand
2-Acetylpyridine	1122-62-9	C ₇ H ₇ NO	121.14 (MW)	AR	Aladdin
Iodine	7553-56-2	I ₂	253.81 (MW)	AR	Aladdin
Pyridine	110-86-1	C ₅ H ₅ N	79.10 (FW)	AR	SCR
Acetone	67-64-1	C ₃ H ₆ O	58.08 (FW)	AR	SCR

Step 2: Synthesis of (+)-Myrtenal.



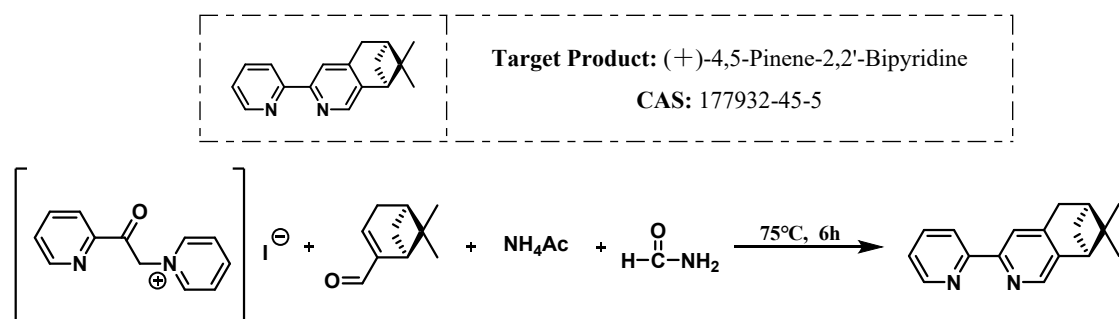
80 mL of dichloromethane and 62 mL of tert-butyl hydroperoxide 70% aqueous solution were measured in a partition funnel and shaken and left to extract. The lower liquid (organic phase) was poured into a 250 mL two-necked round-bottom flask containing 0.52 g SeO₂. Stirring at room temperature, SeO₂ was dissolved and then heated up to 35 °C. After 20.45 mL of (+)- α -pinene was slowly (approximately 2 h) dropped into the reaction solution with a constant pressure dropping funnel, the reaction was carried out for 48 h. After the reaction, the reaction mixture was washed with 60 mL of dilute KOH aqueous solution, and then washed with saturated NaCl aqueous solution to neutral. The organic phase was dried with anhydrous Na₂SO₄. After suction filtration, the solvent was removed by rotary-evaporation to obtain a dark yellow cloudy crude product. The product was collected by elution with absolute ether/petroleum ether = 1:10 (v/v) over the column, and the product was obtained as a pale-yellow liquid product after spin evaporation (yield 25.7%).

Table S3. The information on used chemicals in *step 2*.

Chemical	CAS	Formula	MW / FW	Purity Level	Brand
tert-Butyl Hydroperoxide (t-BuOOH)	75-91-2	C ₄ H ₁₀ O ₂	90.12 (MW)	70% aqueous solution	Acros
Selenium Dioxide	7446-08-4	SeO ₂	110.96 (MW)	AR	Aladdin
Dichloromethane	75-09-2	CH ₂ Cl ₂	84.93 (FW)	AR	SCR

(+)- α -Pinene	7785-70-8	C ₁₀ H ₁₆	136.24 (MW)	AR	Aladdin
Potassium Hydroxide	1310-58-3	KOH	56.11 (MW)	AR	SCR
Sodium Chloride	7647-14-5	NaCl	58.44 (MW)	AR	SCR
Sodium Sulfate	7757-82-6	Na ₂ SO ₄	142.04 (MW)	AR	SCR
Petroleum Ether 60-90 °C	8032-32-4	C ₅ H ₁₂ O ₂	195.34 (FW)	AR	SCR
Absolute Ether	60-29-7	C ₄ H ₁₀ O	74.12 (FW)	AR	SCR

Step 3: Synthesis of (+)-4,5-Pinene-2,2'-Bipyridine.



6.5 g 1-[2-oxo-2-(2-pyridyl)ethyl]pyridinium iodide (*precursor 1*), 3.0 g (+)-myrtenal (*precursor 2*), 3.1 g ammonium acetate and 30 mL formamide were added to a 100 mL round-bottom flask and refluxed at 75 °C for 6 h. After the reaction, 30 mL of water was added immediately. The mixture was stirred continuously for 30 s and cooled to room temperature. Multiple extractions were performed with hexane, and the organic phases were combined, dried with anhydrous Na₂SO₄, suction filtered by extraction, and rotary-evaporated to get a brownish crude product. Multiple extractions were performed with hexane, and the organic phases were combined, dried with anhydrous Na₂SO₄, suction filtered by extraction, and rotary-evaporated to get a brownish crude product. The product was eluted with 400 mL of absolute ether/petroleum ether = 1:50 (v/v), and the fraction was not collected in this step; then eluted with 300 mL of triethylamine/hexane/ethyl acetate = 1:4.5:4.5 (v/v), and the fraction was collected and rotary-evaporated to obtain a yellowish-brown solid product, which was dried under vacuum, washed with acetone by filtration, and dried to obtain a light-yellow solid. The light-yellow solid was redissolved in a small amount of acetone and recrystallized at room temperature to obtain colorless block crystals (yield: 32.7%).

Table S4. The information on used chemicals in *step 3*.

Chemical	CAS	Formula	MW / FW	Purity Level	Brand
1-[2-Oxo-2-(2-pyridyl)ethyl]pyridinium Iodide	26482-00-8	C ₁₂ H ₁₁ N ₂ OI	326.20 (MW)	/	<i>precursor 1</i>
(+)-Myrtenal	23727-16-4	C ₁₀ H ₁₄ O	150.22 (MW)	/	<i>precursor 2</i>
Ammonium Acetate	631-61-8	C ₂ H ₇ O ₂ N	77.08 (FW)	AR	SCR
Formamide	75-12-7	CH ₃ NO	45.04 (MW)	AR	Aladdin
Hexane	110-54-3	C ₆ H ₁₄	86.18 (FW)	AR	SCR
Sodium Sulfate	7757-82-6	Na ₂ SO ₄	142.04 (MW)	AR	SCR
Petroleum Ether 60-90 °C	8032-32-4	C ₅ H ₁₂ O ₂	195.34 (FW)	AR	SCR
Absolute Ether	60-29-7	C ₄ H ₁₀ O	74.12 (FW)	AR	SCR
Triethylamine	121-44-8	C ₆ H ₁₅ N	101.19 (FW)	AR	SCR
Ethyl acetate	141-78-6	C ₄ H ₈ O ₂	88.11 (FW)	AR	SCR

Synthesis of (-)-4,5-Pinene-2,2'-Bipyridine

Because (-)-myrtenal is purchased commercially, the synthesis of (-)-4,5-pinene-2,2'-bipyridine requires only two steps. The **step 1** is exactly the same as *the step 1 above*, and the difference between the **step 2** and *the step 3 above* is only the replacement of the (+)-myrtenal with (-)-myrtenal (CAS: 18486-69-6, Aladdin), yield is 48.5%.

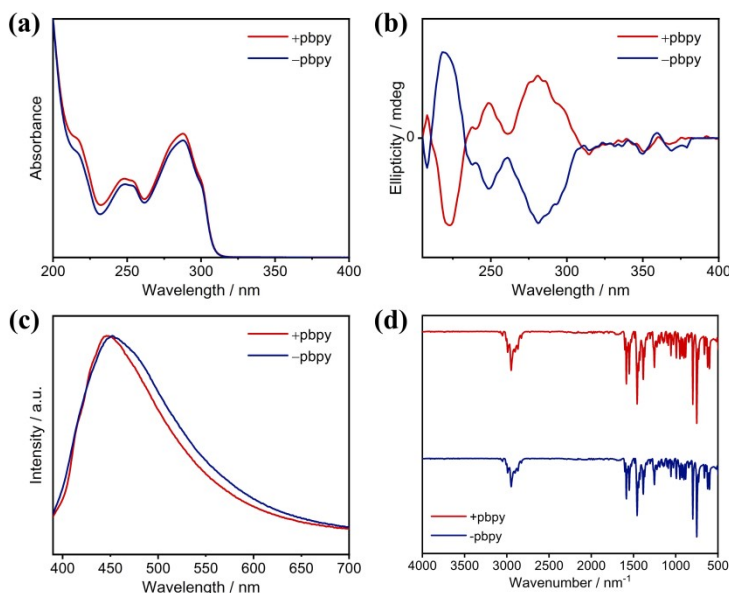


Fig. S1 (a) The UV–vis absorption spectra of 4,5-pinene-2,2'-bipyridine enantiomers; (b) The CD spectra of 4,5-pinene-2,2'-bipyridine enantiomers; (c) The emission spectra of 4,5-pinene-2,2'-bipyridine enantiomers; (d) The FT-IR of 4,5-pinene-2,2'-bipyridine enantiomers.

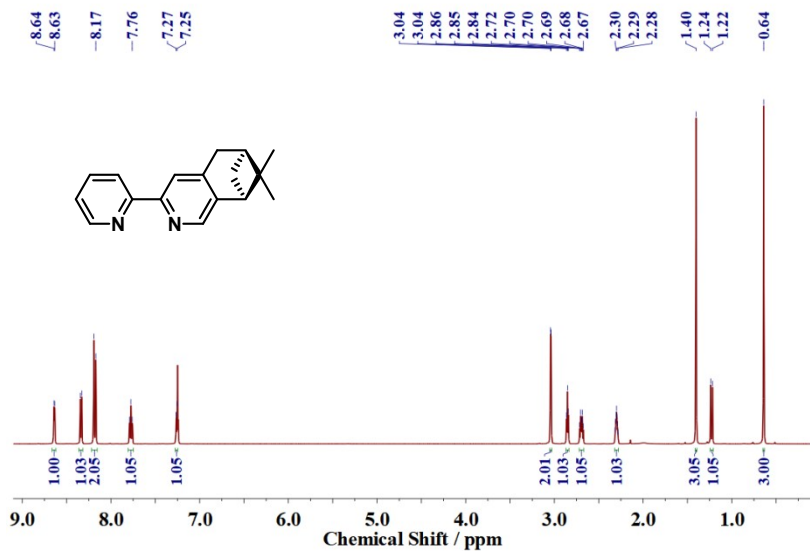


Fig. S2 The ^1H NMR spectrometry of (+)-4,5-pinene-2,2'-bipyridine.

^1H NMR (500 MHz, CDCl_3) δ 8.64 (d, $J = 4.2$ Hz, 1H), 8.64 (d, $J = 4.2$ Hz, 1H), 8.34 (d, $J = 8.0$ Hz, 1H), 8.34 (d, $J = 8.0$ Hz, 1H), 8.18 (d, $J = 10.9$ Hz, 2H), 8.18 (d, $J = 10.9$ Hz, 2H), 7.78 (t, $J = 7.7$ Hz, 1H), 7.78 (t, $J = 7.7$ Hz, 1H), 7.26 (d, $J = 5.9$ Hz, 1H), 3.04 (d, $J = 2.3$ Hz, 2H), 3.04 (d, $J = 2.3$ Hz, 2H), 2.85 (t, $J = 5.5$ Hz, 1H), 2.85 (t, $J = 5.5$ Hz, 1H), 2.69 (dt, $J = 9.7, 5.8$ Hz, 1H), 2.69 (dt, $J = 9.7, 5.8$ Hz, 1H), 2.30 (dq, $J = 8.4, 2.7$ Hz, 1H), 2.30 (dq, $J = 8.4, 2.7$ Hz, 1H), 1.40 (s, 3H), 1.40 (s, 3H), 1.23 (d, $J = 9.6$ Hz, 1H), 1.23 (d, $J = 9.6$ Hz, 1H), 0.64 (s, 3H), 0.64 (s, 3H).

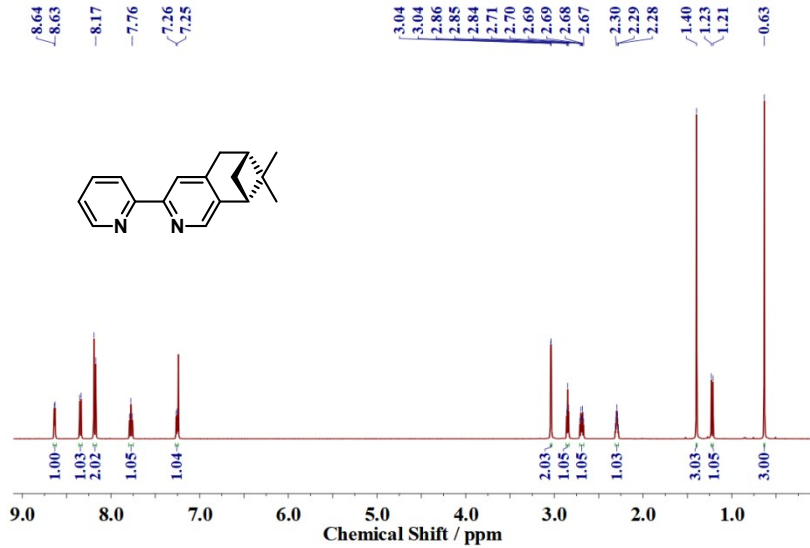


Fig. S3 The ^1H NMR spectrometry of (-)-4,5-pinene-2,2'-bipyridine.

^1H NMR (500 MHz, CDCl_3) δ 8.63 (d, $J = 4.1$ Hz, 1H), 8.63 (d, $J = 4.1$ Hz, 1H), 8.34 (d, $J = 8.0$ Hz, 1H), 8.34 (d, $J = 8.0$ Hz, 1H), 8.18 (d, $J = 9.9$ Hz, 2H), 8.18 (d, $J = 9.9$ Hz, 2H), 7.78 (t, $J = 7.7$ Hz, 1H), 7.78 (t, $J = 7.7$ Hz, 1H), 7.26 (d, $J = 4.9$ Hz, 1H), 7.26 (d, $J = 4.9$ Hz, 1H), 3.04 (d, $J = 2.6$ Hz, 2H), 3.04 (d, $J = 2.6$ Hz, 2H), 2.85 (t, $J = 5.5$ Hz, 1H), 2.85 (t, $J = 5.5$ Hz, 1H), 2.69 (dt, $J = 9.7, 5.8$ Hz, 1H), 2.69 (dt, $J = 9.7, 5.8$ Hz, 1H), 2.30 (tt, $J = 5.7, 2.8$ Hz, 1H), 2.30 (tt, $J = 5.7, 2.8$ Hz, 1H), 1.40 (s, 3H), 1.40 (s, 3H), 1.22 (d, $J = 9.6$ Hz, 1H), 1.22 (d, $J = 9.6$ Hz, 1H), 0.63 (s, 3H), 0.63 (s, 3H).

Table S5. Single crystal structure refinements of 4,5-pinene-2,2'-bipyridine enantiomers.

Chiral enantiomers	(+)-4,5-pinene-2,2'-bipyridine	(-)-4,5-pinene-2,2'-bipyridine
CCDC	2214390	2214391
Formula	C ₁₇ H ₁₈ N ₂	C ₁₇ H ₁₈ N ₂
<i>M_r</i>	250.33	250.33
Temperature/K	99.9(9)	100.0(8)
Crystal color	colorless	colorless
Crystal system	orthorhombic	orthorhombic
Space group	<i>P</i> 2 ₁ 2 ₁ 2 ₁	<i>P</i> 2 ₁ 2 ₁ 2 ₁
<i>a</i> /Å	9.18000(10)	9.18570(10)
<i>b</i> /Å	9.95850(10)	9.18570(10)
<i>c</i> /Å	14.79740(10)	14.77970(10)
$\alpha/^\circ$	90	90
$\beta/^\circ$	90	90
$\gamma/^\circ$	90	90
<i>V</i> /Å ³	1352.76(2)	1351.01(2)
<i>Z</i>	4	4
$\rho_{\text{calc}}/\text{g}\cdot\text{cm}^{-3}$	1.229	1.231
μ/mm^{-1}	0.558	0.558
2θ range/°	10.708-150.254	10.718 to 150.158
Reflections collected	29957	29776
Data/restraints/parameters	2669/0/174	2680/0/174
Goodness-of-fit on F ²	1.088	1.082
Final R indexes [I>=2σ (I)] ^a	R ₁ = 0.0292, wR ₂ = 0.0732	R ₁ = 0.0279, wR ₂ = 0.0710
Final R indexes [all data] ^b	R ₁ = 0.0292, wR ₂ = 0.0733	R ₁ = 0.0280, wR ₂ = 0.0711
Flack parameter	0.11(7)	0.05(8)

^aR₁ = $\sum(|F_o| - |F_c|) / \sum |F_o|$; ^bwR₂ = $\{\sum [w(F_o^2 - F_c^2)^2] / \sum [w(F_o^2)^2]\}^{1/2}$;

w = 1/[²(F_o)²+(aP)²+bP] and P = (F_o²+2F_c²)/3.

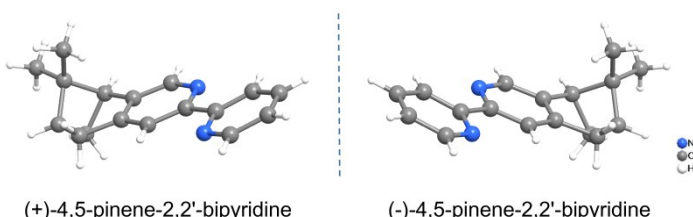


Fig. S4 The crystal structures of 4,5-pinene-2,2'-bipyridine enantiomers.

Synthesis and characteristics of chiral europium-titanium-oxo clusters.

Chemicals. In the synthesis process of the used analytically pure europium acetate hydrate ($\text{Eu(OAc)}_3 \cdot x\text{H}_2\text{O}$), pivalic acid (Hpa), benzoic acid (Hba), 4-tert-butylbenzoic acid (4-Htbba), titanium tetraisopropanolate ($\text{Ti(O}^i\text{Pr)}_4$) and acetonitrile (MeCN) are all the commercial sources and were received without further purification. The pair of chiral ligands (+)-4,5-pinene-2,2'-bipyridine (+pbpy) and (-)-4,5-pinene-2,2'-bipyridine (-pbpy) were synthesized according to the above procedures by self.

Table S6. The information on used chemicals in the synthesis process of **1-6**.

Chemical	CAS	Formula	MW / FW	Purity Level	Brand
Europium Acetate Hydrate ($\text{Eu(OAc)}_3 \cdot x\text{H}_2\text{O}$)	62667-64-5	$\text{Eu(OOCCH}_3)_3 \cdot x\text{H}_2\text{O}$	329.10 (MW)	AR	Aladdin
Titanium Tetraisopropanolate ($\text{Ti(O}^i\text{Pr)}_4$)	546-68-9	$\text{Ti}[\text{OCH(CH}_3)_2]_4$	284.23 (FW)	AR	Alfa Aesar
Pivalic Acid	75-98-9	$(\text{CH}_3)_3\text{CCOOH}$	102.13 (MW)	AR	Aladdin
Benzoic Acid	65-85-0	$\text{C}_6\text{H}_5\text{COOH}$	122.12 (MW)	AR	Aladdin
4-tert-Butylbenzoic Acid	98-73-7	$(\text{CH}_3)_3\text{CC}_6\text{H}_4\text{COOH}$	178.23 (MW)	AR	Aladdin
(+)-4,5-Pinene-2,2'-Bipyridine	177932-45-5	$\text{C}_{17}\text{H}_{18}\text{N}_2$	250.34 (MW)	/	/
(-)-4,5-Pinene-2,2'-Bipyridine	144176-23-8	$\text{C}_{17}\text{H}_{18}\text{N}_2$	250.34 (MW)	/	/
Acetonitrile (MeCN)	75-05-8	CH_3CN	41.05 (FW)	AR	SCR

Synthesis of **1-6**.

$\text{Eu}_2\text{Ti}_4(\mu_2\text{-O})_2(\mu_3\text{-O})_4(+\text{pbpy})_2(\text{pa})_{10}$ (1) $\text{Eu(OAc)}_3 \cdot x\text{H}_2\text{O}$ (16.5 mg, 0.05 mmol), pivalic acid (Hpa, 76.6 mg, 0.75 mmol), (+)-4,5-pinene-2,2'-bipyridine (+pbpy, 17.5 mg, 0.07 mmol) and 4 mL MeCN were added to an 8 mL vial. Then $\text{Ti(O}^i\text{Pr)}_4$ (15 μL , 0.05 mmol) was added dropwise into the above mixture. The new mixture was sealed and sonicated for 5 min. Colorless block-shaped crystals were obtained after 2 days in a 80 °C temperature environment (37.6% yield based on $\text{Eu(OAc)}_3 \cdot x\text{H}_2\text{O}$). Anal. Calcd for $\text{C}_{84}\text{H}_{126}\text{O}_{26}\text{N}_6\text{Eu}_2\text{Ti}_4$ (FW = 2103.40): C, 47.96; H, 6.03; O, 19.78; N, 2.66 (%); Found: C, 48.09; H, 6.05; O, 19.67; N, 2.71 (%).

$\text{Eu}_2\text{Ti}_4(\mu_2\text{-O})_2(\mu_3\text{-O})_4(-\text{pbpy})_2(\text{pa})_{10}$ (2) was synthesized by the same method as **1** except the substitution of (+)-4,5-pinene-2,2'-bipyridine to (-)-4,5-pinene-2,2'-bipyridine (-pbpy). Colorless block-shaped crystals were obtained (36.4% yield based on $\text{Eu(OAc)}_3 \cdot x\text{H}_2\text{O}$). Anal. Calcd for $\text{C}_{84}\text{H}_{126}\text{O}_{26}\text{N}_6\text{Eu}_2\text{Ti}_4$ (FW = 2103.40): C, 47.96; H, 6.03; O, 19.78; N, 2.66 (%); Found: C, 48.05; H, 6.06; O, 19.73; N, 2.68 (%).

Eu₂Ti₄(μ₂-O)₂(μ₃-O)₄(+pbpy)₂(ba)₁₀ (3) Eu(OAc)₃·xH₂O (16.5 mg, 0.05 mmol), benzoic acid (Hba, 122.1 mg, 1.00 mmol), (+)-4,5-pinene-2,2'-bipyridine (+pbpy, 25.0 mg, 0.10 mmol) and 5 mL MeCN were added to an 8 mL vial. Then Ti(O*i*Pr)₄ (36 μL, 0.12 mmol) was added dropwise into the above mixture. The new mixture was sealed and sonicated for 5 min. Colorless block-shaped crystals were obtained after 2 days in a 80 °C temperature environment (42.6% yield based on Eu(OAc)₃·xH₂O). Anal. Calcd for C₁₀₄H₈₆O₂₆N₆Eu₂Ti₄ (FW = 2303.28): C, 54.23; H, 3.76; O, 18.06; N, 2.43 (%); Found: C, 54.25; H, 3.73; O, 18.16; N, 2.48 (%).

Eu₂Ti₄(μ₂-O)₂(μ₃-O)₄(-pbpy)₂(ba)₁₀ (4) was synthesized by the same method as **3** except the substitution of (+)-4,5-pinene-2,2'-bipyridine to (-)-4,5-pinene-2,2'-bipyridine (-pbpy). Colorless block-shaped crystals were obtained (43.4% yield based on Eu(OAc)₃·xH₂O). Anal. Calcd for C₁₀₄H₈₆O₂₆N₆Eu₂Ti₄ (FW = 2303.28): C, 54.23; H, 3.76; O, 18.06; N, 2.43 (%); Found: C, 54.26; H, 3.77; O, 18.14; N, 2.47 (%).

Eu₂Ti₄(μ₂-O)₂(μ₃-O)₄(+pbpy)₂(4-tbba)₁₀ (5) Eu(OAc)₃·xH₂O (16.5 mg, 0.05 mmol), 4-tert-butylbenzoic acid (4-Htbba, 142.56 mg, 0.80 mmol), (+)-4,5-pinene-2,2'-bipyridine (+pbpy, 25.0 mg, 0.10 mmol) and 4 mL MeCN were added to an 8 mL vial. Then Ti(O*i*Pr)₄ (36 μL, 0.12 mmol) was added dropwise into the above mixture. The new mixture was sealed and sonicated for 5 min. Colorless block-shaped crystals were obtained after 2 days in a 80 °C temperature environment (40.8% yield based on Eu(OAc)₃·xH₂O). Anal. Calcd for C₁₄₄H₁₆₆O₂₆N₄Eu₂Ti₄ (FW = 2864.32): C, 60.38; H, 5.83; O, 14.52; N, 1.96 (%); Found: C, 60.43; H, 5.85; O, 14.59; N, 1.97 (%).

Eu₂Ti₄(μ₂-O)₂(μ₃-O)₄(-pbpy)₂(4-tbba)₁₀ (6) was synthesized by the same method as **5** except the substitution of (+)-4,5-pinene-2,2'-bipyridine to (-)-4,5-pinene-2,2'-bipyridine (-pbpy). Colorless block-shaped crystals were obtained (41.4% yield based on Eu(OAc)₃·xH₂O). Anal. Calcd for C₁₄₄H₁₆₆O₂₆N₄Eu₂Ti₄ (FW = 2864.32): C, 60.38; H, 5.83; O, 14.52; N, 1.96 (%); Found: C, 60.40; H, 5.88; O, 14.61; N, 1.99 (%).

Table S7. Single crystal structure refinements of **1&2**.

Clusters	1	2
CCDC	2214392	2214393
Formula	C ₈₄ H ₁₂₆ O ₂₆ N ₆ Eu ₂ Ti ₄	C ₈₄ H ₁₂₆ O ₂₆ N ₆ Eu ₂ Ti ₄
<i>M_r</i>	2103.40	2103.40
Temperature/K	100.00(10)	99.99(10)
Crystal color	colorless	colorless
Crystal system	monoclinic	monoclinic
Space group	<i>C2</i>	<i>C2</i>
<i>a</i> /Å	26.7869(10)	26.861(3)
<i>b</i> /Å	15.6539(4)	15.6451(9)
<i>c</i> /Å	14.6425(6)	14.6838(17)
$\alpha/^\circ$	90	90
$\beta/^\circ$	125.081(6)	125.433(15)
$\gamma/^\circ$	90	90
<i>V</i> /Å ³	5024.5(4)	5027.9(11)
<i>Z</i>	2	2
ρ_{calc} /g·cm ⁻³	1.390	1.389
μ /mm ⁻¹	11.935	11.927
2θ range/°	6.938-155.958	6.946 to 152.006
Reflections collected	35765	37152
Data/restraints/parameters	9962/415/688	9428/657/696
Goodness-of-fit on F ²	1.073	1.093
Final R indexes [I>=2σ (I)] ^a	R ₁ = 0.0576, wR ₂ = 0.1566	R ₁ = 0.0686, wR ₂ = 0.1869
Final R indexes [all data] ^b	R ₁ = 0.0673, wR ₂ = 0.1645	R ₁ = 0.0884, wR ₂ = 0.2039
Flack parameter	0.085(12)	0.070(12)

^aR₁ = $\sum(|F_o| - |F_c|) / \sum |F_o|$; ^bwR₂ = $\{\sum [w(F_o^2 - F_c^2)^2] / \sum [w(F_o^2)^2]\}^{1/2}$;

w = 1/[²(F_o)²+(aP)²+bP] and P = (F_o²+2F_c²)/3.

Table S8. Single crystal structure refinements of **3&4**.

Clusters	3	4
CCDC	2214394	2214395
Formula	C ₁₀₄ H ₈₆ O ₂₆ N ₆ Eu ₂ Ti ₄	C ₁₀₄ H ₈₆ O ₂₆ N ₆ Eu ₂ Ti ₄
M _r	2303.28	2303.28
Temperature/K	100.01(13)	100.00(13)
Crystal color	colorless	colorless
Crystal system	triclinic	triclinic
Space group	P1	P1
a/Å	13.1002(2)	13.0912(3)
b/Å	14.6924(2)	14.7170(4)
c/Å	15.1253(2)	15.1448(4)
α/°	67.479(2)	67.337(3)
β/°	89.6700(10)	89.583(2)
γ/°	73.051(2)	73.074(2)
V/Å ³	2553.86(8)	2557.66(13)
Z	1	1
ρ _{calc} /g·cm ⁻³	1.498	1.495
μ/mm ⁻¹	11.810	11.792
2θ range/°	6.372-152.122	6.37-148.65
Reflections collected	36250	32698
Data/restraints/parameters	13766/993/1373	13819/1170/1432
Goodness-of-fit on F ²	1.106	1.069
Final R indexes [I>=2σ (I)] ^a	R ₁ = 0.0494, wR ₂ = 0.1343	R ₁ = 0.0619, wR ₂ = 0.1695
Final R indexes [all data] ^b	R ₁ = 0.0565, wR ₂ = 0.1405	R ₁ = 0.0654, wR ₂ = 0.1734
Flack parameter	0.045(6)	0.052(6)

^aR₁ = $\sum(|F_o| - |F_c|) / \sum |F_o|$; ^bwR₂ = $\{\sum [w(F_o^2 - F_c^2)^2] / \sum [w(F_o^2)^2]\}^{1/2}$;

w = 1/[²(F_o)²+(aP)²+bP] and P = (F_o²+2F_c²)/3.

Table S9. Single crystal structure refinements of **5&6**.

Clusters	5	6
CCDC	2214396	2214397
Formula	C ₁₄₄ H ₁₆₆ O ₂₆ N ₄ Eu ₂ Ti ₄	C ₁₄₄ H ₁₆₆ O ₂₆ N ₄ Eu ₂ Ti ₄
<i>M_r</i>	2864.32	2864.32
Temperature/K	100.00(13)	100.00(13)
Crystal color	colorless	colorless
Crystal system	triclinic	triclinic
Space group	<i>P</i> 1	<i>P</i> 1
<i>a</i> /Å	16.46530(10)	17.4057(2)
<i>b</i> /Å	18.56690(10)	21.3759(3)
<i>c</i> /Å	26.3060(2)	22.6058(3)
$\alpha/^\circ$	76.7580(10)	89.6750(10)
$\beta/^\circ$	81.8710(10)	75.5190(10)
$\gamma/^\circ$	78.6230(10)	70.3620(10)
<i>V</i> /Å ³	7635.24(10)	7641.52(18)
<i>Z</i>	2	2
ρ_{calc} /g·cm ⁻³	1.246	1.245
μ /mm ⁻¹	7.996	7.989
2θ range/°	3.468-154.524	4.052-148.912
Reflections collected	278762	104418
Data/restraints/parameters	57733/3694/3309	39672/4970/3694
Goodness-of-fit on F ²	1.088	1.073
Final R indexes [I>=2σ (I)] ^a	R ₁ = 0.0473, wR ₂ = 0.1203	R ₁ = 0.0320, wR ₂ = 0.0808
Final R indexes [all data] ^b	R ₁ = 0.0527, wR ₂ = 0.1233	R ₁ = 0.0348, wR ₂ = 0.0820
Flack parameter	0.054(3)	0.040(2)

^aR₁ = $\sum(|F_o| - |F_c|) / \sum |F_o|$; ^bwR₂ = $\{\sum [w(F_o^2 - F_c^2)^2] / \sum [w(F_o^2)^2]\}^{1/2}$;

w = 1/[²(F_o)²+(aP)²+bP] and P = (F_o²+2F_c²)/3.

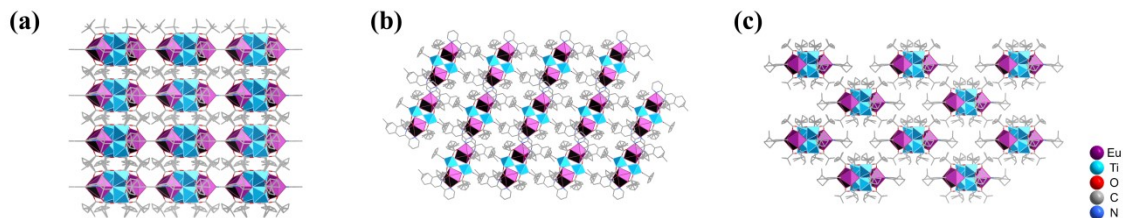


Figure S5. The packing structures of **1** in (a) a-axis, (b) b-axis and (c) c-axis.

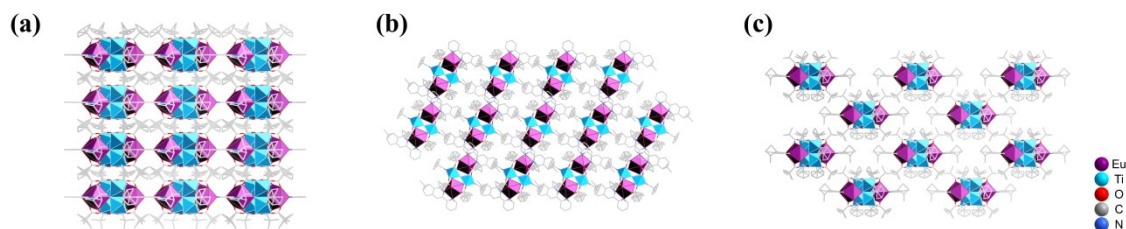


Fig. S6 The packing structures of **2** in (a) a-axis, (b) b-axis and (c) c-axis.

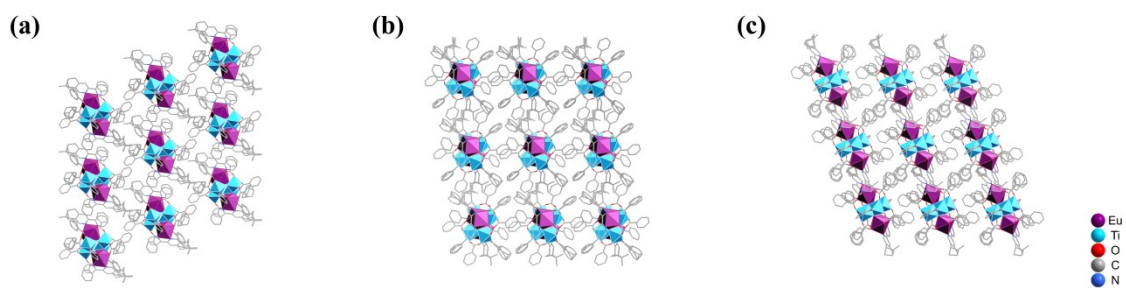


Fig. S7 The packing structures of **3** in (a) a-axis, (b) b-axis and (c) c-axis.

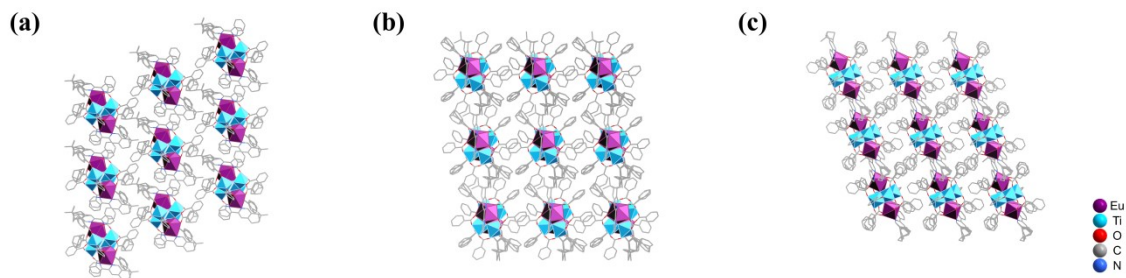


Fig. S8 The packing structures of **4** in (a) a-axis, (b) b-axis and (c) c-axis.

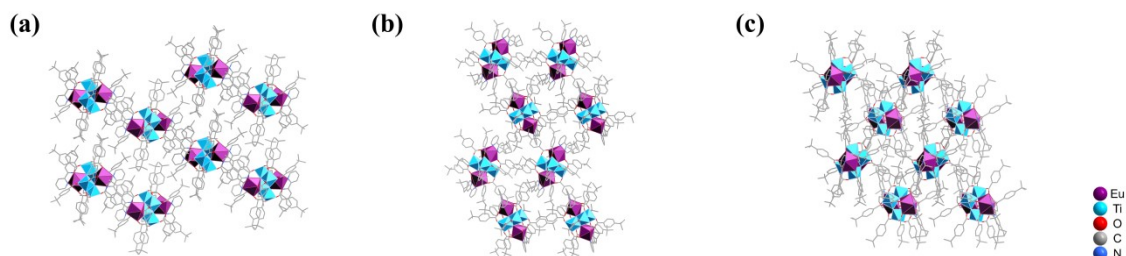


Fig. S9 The packing structures of **5** in (a) a-axis, (b) b-axis and (c) c-axis.

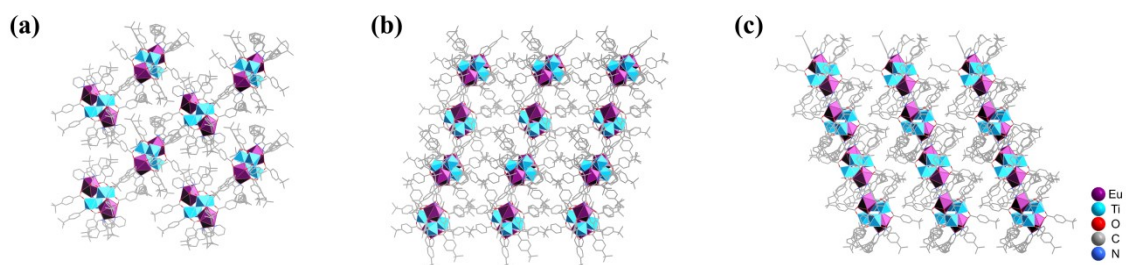


Fig. S10 The packing structures of **6** in (a) a-axis, (b) b-axis and (c) c-axis.

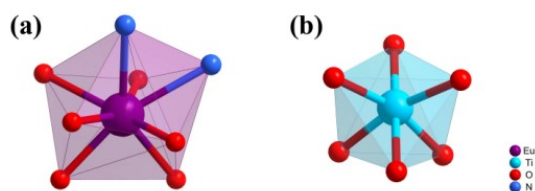


Fig. S11 The coordination configurations of (a) Eu^{3+} ions in **1-6**; (b) Ti^{4+} ions in **1-6**. The Eu^{3+} ions are all eight-coordinated with six O atoms and two N atoms in **1-6**. The Ti^{4+} ions are all six-coordinated with six O atoms in **1-6**.

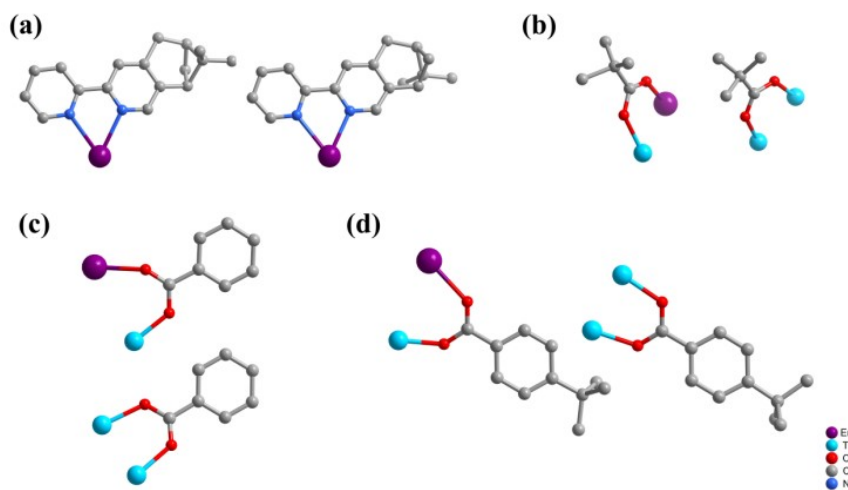


Fig. S12 Coordination modes of (a) chiral pbpy ligands in **1-6**; (b) pa^- ligands in **1&2**; (c) ba^- ligands in **3&4**; (d) 4-tbba $^-$ ligands in **5&6**.

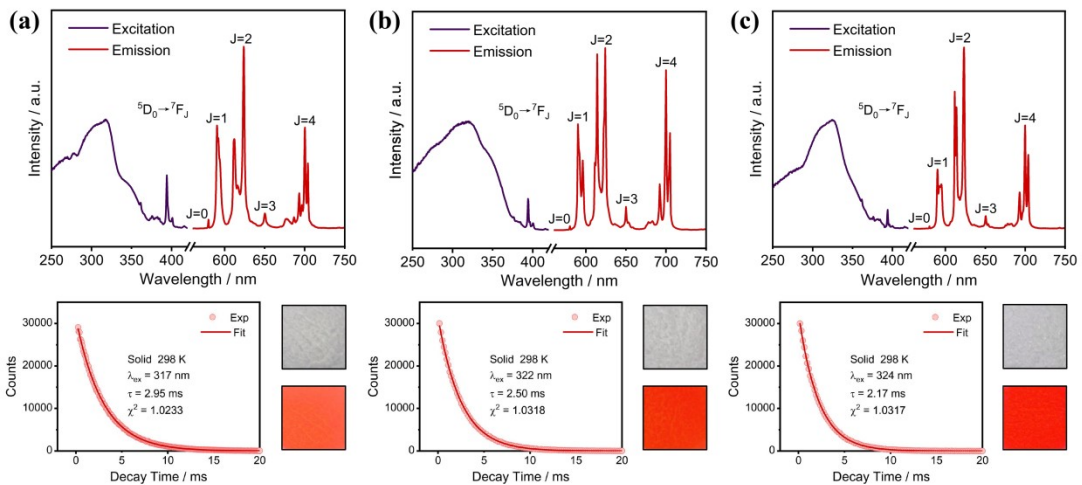


Fig. S13 (a-c) Excitation and emission spectra, the excited-state decay curves and physical photographs of **2, 4, 6**.

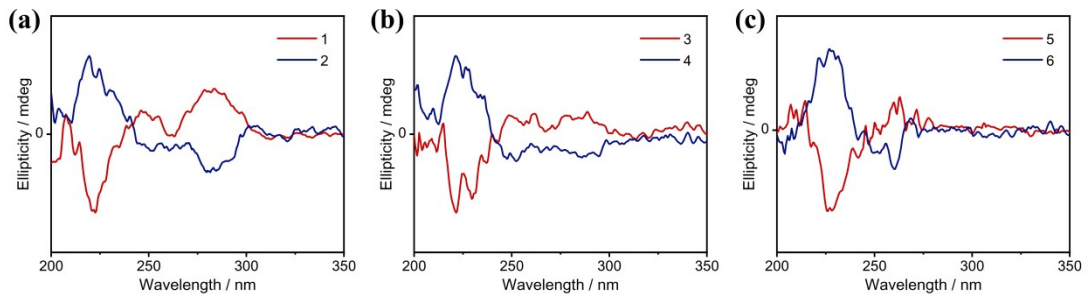


Fig. S14 The CD spectra of (a) **1&2**; (b) **3&4**; (c) **5&6**.

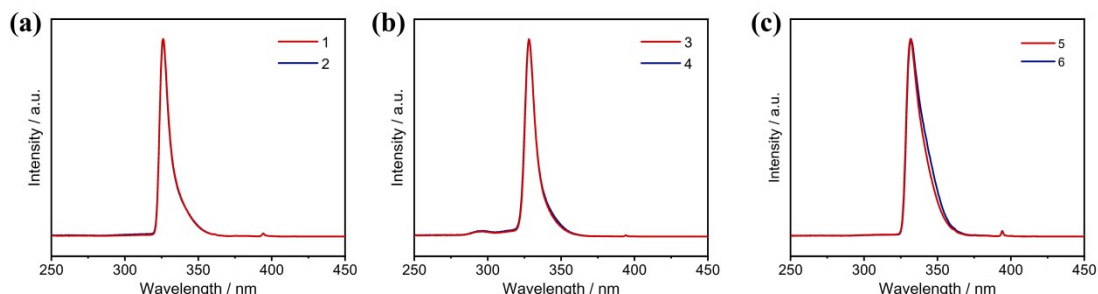


Fig. S15. The excitation spectra of CH₂Cl₂ solutions of (a) **1&2**; (b) **3&4**; (c) **5&6**.

Table S10. List of representative metal-organic CPL emitters

Classification	Compound	Metal Center(s)	$ g_{\text{lum}} $	Ref.
Coordination complexes	Cs[Eu((+)-hfbc) ₄]	Eu ³⁺	1.38	[2]
	Eu(±tfc)-tmpo	Eu ³⁺	1.2	[3]
	Tb-Ph-PyBox	Tb ³⁺	1.4×10 ⁻¹	[4]
	Sm(HFA) ₃ (R)- ⁱ Pr-PyBox	Sm ³⁺	1.8×10 ⁻¹	[5]
	CAACCuCl	Cu ⁺	1.2×10 ⁻³	[6]
	Ir(III)-NHC-helicene complexes	Ir ³⁺	3.7×10 ⁻³	[7]
	[Cr(dqp) ₂] ³⁺	Cr ³⁺	2×10 ⁻¹	[8]
Metal clusters	(R/S)-PtBox/PtN	Pt ²⁺	6.4×10 ⁻²	[9]
	(Au ₄ L ₄) _n /(Au ₄ D ₄) _n	Au ⁺	7×10 ⁻³	[10]
	[Au ₆ (C ₂ C ₁₀ H ₁₇ O) ₄ (PPh ₂ C ₃ H ₆ PPh ₂) ₂](PF ₆) ₂	Au ⁺	6×10 ⁻³	[11]
	Ag ₆ L ₆ /D ₆	Ag ⁺	4.42×10 ⁻³	[12]
	R/S-Ag ₁₇	Ag ⁺	1.2×10 ⁻³	[13]
	[Cu ₁₄ (R/S-DPM) ₈](PF ₆) ₆	Cu ⁺	1×10 ⁻²	[14]
	Cu ₃ (BINAP) ₃ CO ₃ [^t BuSO ₃] ⁻	Cu ⁺	2×10 ⁻²	[15]
Coordination polymers	[Tb ₉ (sal-(S)-Bt) ₁₆ (μ-OH) ₁₀] ⁺ [NO ₃] ⁻	Tb ³⁺	1×10 ⁻²	[16]
	[Eu(+/-tfc) ₃ (dpbp)] _n	Eu ³⁺	1.7×10 ⁻¹	[17]
	DSM@TbBTC MOF	Tb ³⁺	2.5×10 ⁻³	[18]
	R-/S-ZIF	Zn ²⁺	5.5×10 ⁻³	[19]
	Cd-TCPA MOF	Cd ²⁺	2.7×10 ⁻³	[20]
	[Ba ₂ (μ-D/L-pyro) ₂ (μ ₄ -NO ₃) (μ ₃ -form)] _n	Ba ²⁺	1×10 ⁻³	[21]
	[Eu ₄ (L ₁) ₆](OTf) ₁₂	Eu ³⁺	1.6×10 ⁻¹	[22]
Metal-organic cages	(Eu ₄ L ₄)(R/S-BINAPO) ₄	Eu ³⁺	2×10 ⁻¹	[23]
	Zn ₆ L ₆ (SO ₄) ₄ cages	Zn ²⁺	4×10 ⁻³	[24]
	Pd ₄ Ru ₈ (MOC-52)	Pd ²⁺ , Ru ²⁺	3.9×10 ⁻³	[25]
	helical aggregate Cs[Eu((+)-hfbc) ₄]	Eu ³⁺	1.45	[26]
Helicates	Eu ₂ L ₃ (L') ₂	Eu ³⁺	1.12×10 ⁻¹	[27]
	[(R)- or (S)- ⁱ Pr-Pybox] ₈ (Eu ^{III}) ₈ (THP) ₈	Eu ³⁺	1.25	[28]
	ALPHY	Al ³⁺	4×10 ⁻³	[29]
	Zn(Phena-dpm) ₂	Zn ²⁺	2.2×10 ⁻²	[30]
Metallacycles	Pt (II) metallacycles	Pt ²⁺	2.3×10 ⁻³	[31]
	metallacycles M-S/R	Pt ²⁺	1.4×10 ⁻²	[32]
	Eu ₂ (Pt-L) ₂ (L ^{R/S}) ₂	Eu ³⁺	5.8×10 ⁻²	[33]

The main parameter to measure the CPL property (degree of asymmetry) is the luminescence asymmetry factor (g_{lum} , $-2 \leq g_{lum} \leq 2$):

$$g_{lum} = \frac{\Delta I}{I} = \frac{I_L - I_R}{I_L + I_R} = \frac{2(I_L - I_R)}{I_L + I_R}$$

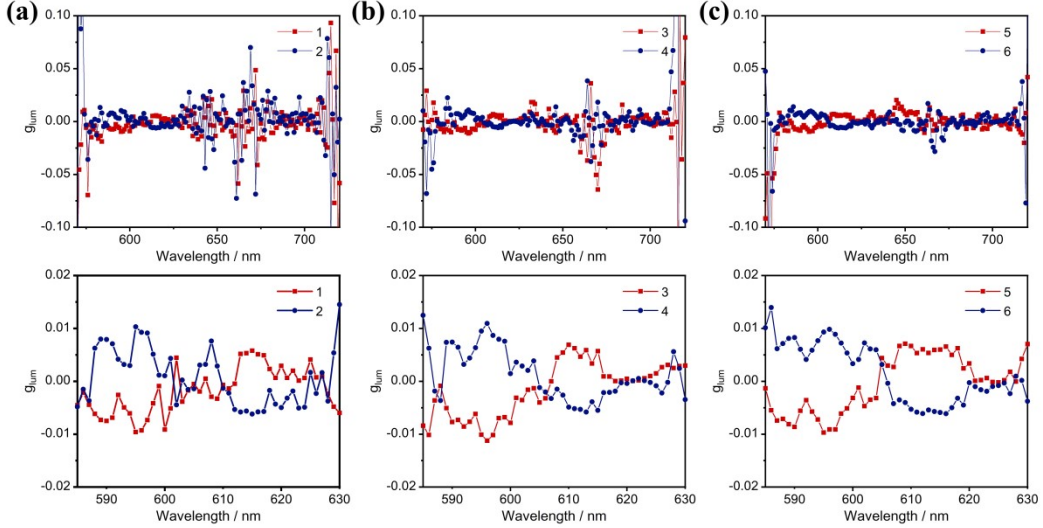


Fig. S16 The g_{lum} versus wavelength of (a) 1&2; (b) 3&4; (c) 5&6.

Table S11. Correspondence between g_{lum} and wavelengths of 1-6.

Clusters	Wavelength (7F_J)	g_{lum}	Clusters	Wavelength (7F_J)	g_{lum}
1	590 nm (J=1)	-0.0082	2	590 nm (J=1)	0.0089
	595 nm (J=1)	-0.0096		595 nm (J=1)	0.0103
	615 nm (J=2)	0.0058		615 nm (J=2)	-0.0062
3	590 nm (J=1)	-0.0091	4	590 nm (J=1)	0.0084
	595 nm (J=1)	-0.0101		595 nm (J=1)	0.0095
	615 nm (J=2)	0.0057		615 nm (J=2)	-0.0055
5	590 nm (J=1)	-0.0086	6	590 nm (J=1)	0.0083
	595 nm (J=1)	-0.0097		595 nm (J=1)	0.0093
	615 nm (J=2)	0.0060		615 nm (J=2)	-0.0059

The $|g_{lum}|$ values for ${}^5D_0 \rightarrow {}^7F_1$ transitions of 1-6 are all determined to be approximately 1×10^{-2} , and for ${}^5D_0 \rightarrow {}^7F_2$ transitions of 1-6 are all found to be approximately 6×10^{-3} . Compared to other metal-organic CPL emitters, the g_{lum} values we observed are moderate.

The B_{CPL} (CPL brightness) of the selected lanthanide transition is calculated following this equation provide by Francesco Zinna [34]:

$$B_{CPL} = \beta_i \times \varepsilon_\lambda \times \phi \times \frac{|g_{lum}|}{2}$$

β_i : branching ratio of transition

ε_λ : the molar extinction coefficient measured at the excitation wavelength (λ), $\varepsilon_\lambda = A/lc$

ϕ : emission quantum yield

g_{lum} : dissymmetry factor

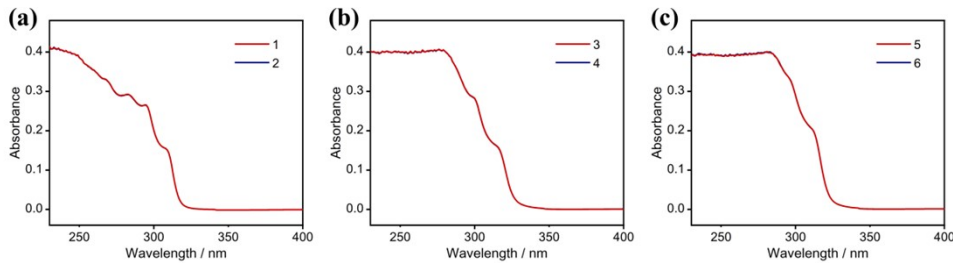


Fig. S17 UV-visible absorption spectra of CH_2Cl_2 solutions of (a) **1&2**; (b) **3&4**; (c) **5&6**.

Concentration of solution (c): 1×10^{-5} M; Cross section size of cuvette: 1 cm \times 1 cm (l).

Table S12. Photophysical parameters and B_{CPL} of CH_2Cl_2 solutions of **1-6**.

Cluster	$\varepsilon / \text{M}^{-1} \cdot \text{cm}^{-1}$ (λ_{abs} / nm)	Φ	7F_J	$ g_{lum} $ (λ / nm)	β	$B_{CPL} / \text{M}^{-1} \cdot \text{cm}^{-1}$
1	1435.9 (326 nm)	0.12	J=1	0.0096 (595 nm)	0.19	0.16
			J=2	0.0058 (615 nm)	0.62	0.31
2	1438.3 (326 nm)	0.10	J=1	0.0103 (595 nm)	0.19	0.14
			J=2	0.0062 (615 nm)	0.62	0.28
3	1258.2 (328 nm)	0.43	J=1	0.0101 (595 nm)	0.20	0.54
			J=2	0.0057 (615 nm)	0.62	0.93
4	1261.8 (328 nm)	0.44	J=1	0.0095 (595 nm)	0.20	0.53
			J=2	0.0055 (615 nm)	0.62	0.94
5	975.1 (332 nm)	0.58	J=1	0.0097 (595 nm)	0.19	0.52
			J=2	0.0060 (615 nm)	0.62	1.05
6	977.8 (332 nm)	0.61	J=1	0.0093 (595 nm)	0.19	0.53
			J=2	0.0059 (615 nm)	0.62	1.09

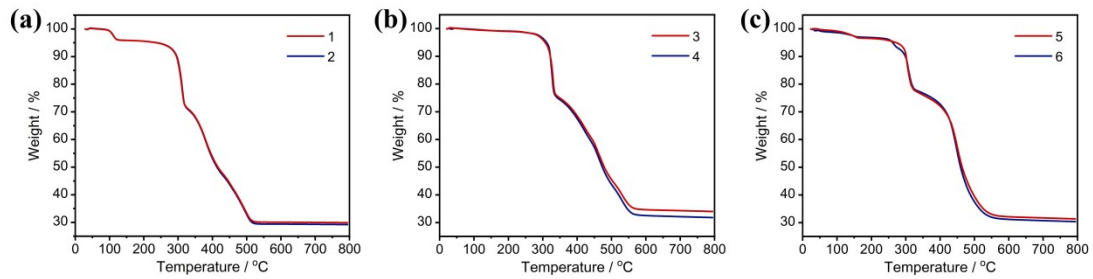


Fig. S18 The TGA curves of (a) 1&2; (b) 3&4; (c) 5&6.

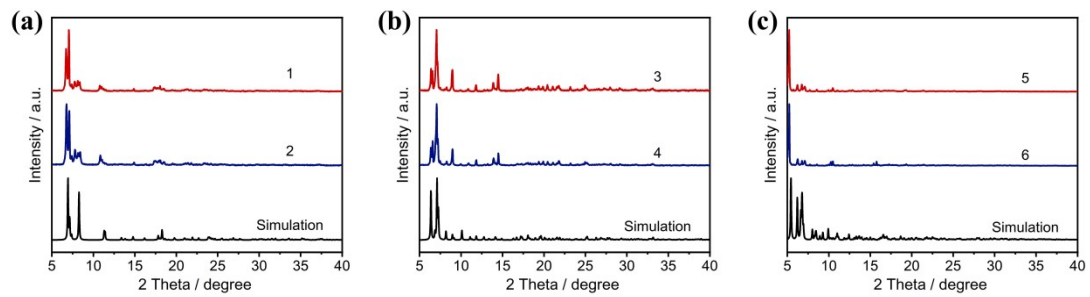


Fig. S19 The PXRD of (a) 1&2; (b) 3&4; (c) 5&6.

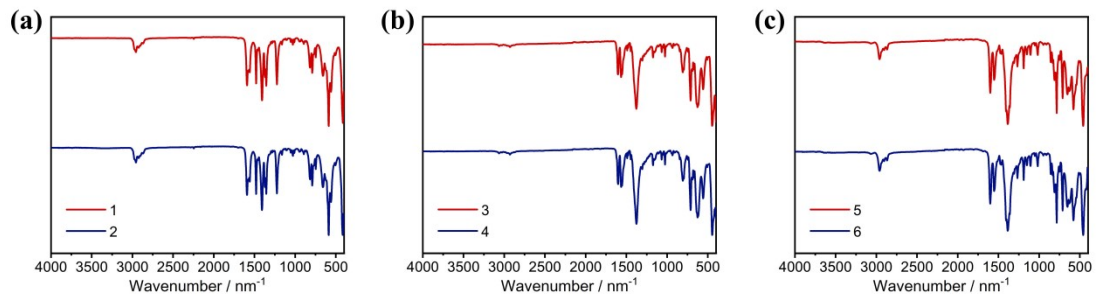


Fig. S20 The FT-IR of (a) 1&2; (b) 3&4; (c) 5&6.

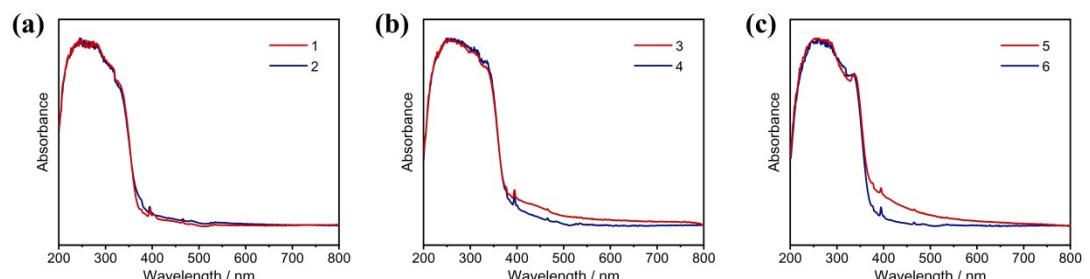


Fig. S21 The DRS of (a) 1&2; (b) 3&4; (c) 5&6.

Table S13. Selected bond distances (\AA) of **1**.

Atom-Atom	Length/ \AA	Atom-Atom	Length/ \AA
Eu1—O6	2.396(5)	Eu1—O8	2.390(10)
Eu1—O5	2.363(10)	Eu1—N1	2.596(7)
Eu1—N4	2.671(1)	Ti1—O1	2.086(10)
Ti1—O6	1.925(9)	Ti1—O10	1.816(5)
Ti1—O14	1.869(10)	Ti1—O9	2.029(10)
Ti1—O3	2.030(9)	Ti2—O4	2.018(10)
Ti2—O6	1.897(10)	Ti2—O12	2.034(11)
Ti2—O14	1.880(10)	Ti2—O11	1.809(5)
Ti2—O13	2.103(10)		

Table S14. Selected bond angles ($^{\circ}$) of **1**.

Atom-Atom-Atom	angles / $^{\circ}$	Atom-Atom-Atom	angles / $^{\circ}$
Ti1—O6—Eu1	122.9(4)	Ti2—O6—Eu1	122.6(4)
Ti2—O6—Ti1	96.0(2)	Ti1—O14—Ti2	98.5(2)

Table S15. Selected bond distances (\AA) of **2**.

Atom-Atom	Length/ \AA	Atom-Atom	Length/ \AA
Eu1—O6	2.355(13)	Eu1—O11	2.419(12)
Eu1—O12	2.395(7)	Eu1—N1	2.666(8)
Eu1—N3	2.595(9)	Ti1—O10	1.823(6)
Ti1—O12	1.898(10)	Ti1—O14	2.032(11)
Ti1—O7	1.881(11)	Ti1—O2	2.011(11)
Ti1—O5	2.096(12)	Ti2—O1	2.098(12)
Ti2—O8	2.029(11)	Ti2—O12	1.910(12)
Ti2—O7	1.880(11)	Ti2—O9	2.021(12)
Ti2—O3	1.805(5)		

Table S16. Selected bond angles ($^{\circ}$) of **2**.

Atom-Atom-Atom	angles / $^{\circ}$	Atom-Atom-Atom	angles / $^{\circ}$
Ti1—O12—Eu1	123.7(5)	Ti2—O12—Eu1	121.4(5)
Ti2—O7—Ti1	98.0(3)	Ti1—O12—Ti2	96.4(3)

Table S17. Selected bond distances (\AA) of **3**.

Atom-Atom	Length/ \AA	Atom-Atom	Length/ \AA
Eu1—O10	2.352(8)	Eu1—O12	2.391(9)
Eu1—O7	2.418(8)	Eu1—O9	2.395(8)
Eu1—N6	2.564(11)	Eu1—N3	2.608(11)
Eu1—O21	2.402(9)	Eu1—O23	2.350(8)
Eu2—O4	2.330(9)	Eu2—O8	2.417(10)
Eu2—O18	2.427(9)	Eu2—O26	2.421(11)
Eu2—N1	2.600(12)	Eu2—N4	2.570(9)
Eu2—O19	2.351(7)	Eu2—O11	2.357(9)
Ti1—O4	1.874(10)	Ti1—O10	1.912(9)
Ti1—O22	2.030(9)	Ti1—O13	2.132(9)
Ti1—O15	2.053(10)	Ti1—O17	1.829(9)
Ti4—O4	1.904(9)	Ti4—O10	1.922(9)
Ti4—O16	1.787(10)	Ti4—O5	2.119(9)
Ti4—O3	2.025(9)	Ti4—O25	2.036(10)
Ti2—O1	2.012(10)	Ti2—O6	2.014(8)
Ti2—O14	2.103(9)	Ti2—O17	1.801(10)
Ti2—O19	1.919(9)	Ti2—O23	1.920(9)
Ti3—O16	1.838(9)	Ti3—O20	2.112(9)
Ti3—O24	2.028(10)	Ti3—O2	2.038(9)
Ti3—O19	1.914(8)	Ti3—O23	1.847(10)

Table S18. Selected bond angles ($^{\circ}$) of 3.

Atom-Atom-Atom	angles / $^{\circ}$	Atom-Atom-Atom	angles / $^{\circ}$
Ti1—O4—Eu2	125.2(4)	Ti1—O4—Ti4	98.1(4)
Ti4—O4—Eu2	124.6(5)	Ti1—O10—Eu2	123.4(4)
Ti1—O10—Ti4	96.2(4)	Ti4—O10—Eu1	122.8(4)
Ti4—O16—Ti3	143.1(5)	Ti2—O17—Ti1	143.3(6)
Ti2—O19—Eu2	122.7(4)	Ti3—O19—Eu2	124.2(4)
Ti3—O19—Ti2	96.7(4)	Ti2—O23—Eu1	122.3(5)
Ti3—O23—Eu1	126.3(4)	Ti3—O23—Ti2	98.9(4)

Table S19. Selected bond distances (\AA) of 4.

Atom-Atom	Length/ \AA	Atom-Atom	Length/ \AA
Eu1—O8	2.453(9)	Eu1—O14	2.330(8)
Eu1—O20	2.351(8)	Eu1—O15	2.416(9)
Eu1—N6	2.568(11)	Eu1—N3	2.599(12)
Eu1—O3	2.422(10)	Eu1—O25	2.366(9)
Eu2—O1	2.375(10)	Eu2—O6	2.414(8)
Eu2—O22	2.373(8)	Eu2—O24	2.400(9)
Eu2—N1	2.617(11)	Eu2—N4	2.557(9)
Eu2—O9	2.336(8)	Eu2—O5	2.380(8)
Ti1—O4	2.021(8)	Ti1—O14	1.898(8)
Ti1—O22	1.932(8)	Ti1—O17	1.782(10)
Ti1—O19	2.022(9)	Ti1—O21	2.090(10)
Ti4—O12	2.045(8)	Ti4—O14	1.871(9)
Ti4—O18	1.841(10)	Ti4—O22	1.895(8)
Ti4—O7	2.138(10)	Ti4—O2	2.015(10)
Ti2—O16	2.110(10)	Ti2—O20	1.916(8)
Ti2—O26	2.034(9)	Ti2—O17	1.834(10)
Ti2—O9	1.868(10)	Ti2—O11	2.031(9)
Ti3—O10	2.122(11)	Ti3—O18	1.796(10)
Ti3—O20	1.905(8)	Ti3—O13	2.021(9)
Ti3—O9	1.913(8)	Ti3—O23	2.016(8)

Table S20. Selected bond angles ($^{\circ}$) of **4**.

Atom-Atom-Atom	angles / $^{\circ}$	Atom-Atom-Atom	angles / $^{\circ}$
Ti1—O14—Eu1	124.7(4)	Ti4—O14—Eu1	125.8(4)
Ti4—O14—Ti1	98.5(4)	Ti3—O18—Ti4	142.6(5)
Ti2—O20—Eu1	124.1(4)	Ti3—O20—Eu1	123.4(4)
Ti3—O20—Ti2	96.7(4)	Ti1—O22—Eu2	123.4(4)
Ti4—O22—Eu2	123.4(4)	Ti4—O22—Ti1	96.5(4)
Ti1—O17—Ti2	143.5(5)	Ti2—O9—Eu2	126.0(4)
Ti2—O9—Eu3	98.1(4)	Ti3—O9—Eu2	123.2(4)

Table S21. Selected bond distances (\AA) of **5**.

Atom-Atom	Length/ \AA	Atom-Atom	Length/ \AA
Eu1—O1	2.386(6)	Eu1—O18	2.432(6)
Eu1—O36	2.329(5)	Eu1—O37	2.372(5)
Eu1—N1	2.598(7)	Eu1—N14	2.581(7)
Eu1—O21	2.375(6)	Eu1—O11	2.415(6)
Eu3—O26	2.405(5)	Eu3—O38	2.358(6)
Eu3—O48	2.358(6)	Eu3—O86	2.335(6)
Eu3—O43	2.404(6)	Eu3—O3	2.400(6)
Eu3—N10	2.558(8)	Eu3—N3	2.609(7)
Ti2—O1	1.912(6)	Ti2—O30	2.087(6)
Ti2—O48	1.887(6)	Ti2—O2	2.056(6)
Ti2—O35	1.825(6)	Ti2—O47	2.079(6)
Ti6—O15	2.029(6)	Ti6—O31	2.047(6)
Ti6—O35	1.800(6)	Ti6—O37	1.899(6)
Ti6—O19	2.120(6)	Ti6—O3	1.889(6)
Ti7—O1	1.918(6)	Ti7—O42	2.110(6)
Ti7—O48	1.893(5)	Ti7—O13	1.799(6)
Ti7—O27	2.021(6)	Ti7—O29	2.039(6)
Ti8—O8	2.072(6)	Ti8—O44	2.037(6)
Ti8—O13	1.833(6)	Ti8—O37	1.856(6)
Ti8—O41	2.086(6)	Ti8—O3	1.902(5)

Table S22. Selected bond angles ($^{\circ}$) of 5.

Atom-Atom-Atom	angles / $^{\circ}$	Atom-Atom-Atom	angles / $^{\circ}$
Ti2—O1—Eu1	125.0(3)	Ti2—O1—Ti7	96.3(3)
Ti7—O1—Eu1	122.2(3)	Ti2—O48—Eu3	124.2(3)
Ti2—O48—Ti7	98.0(3)	Ti7—O48—Eu3	124.6(3)
Ti7—O13—Ti8	142.4(3)	Ti6—O37—Eu1	124.6(3)
Ti8—O37—Eu1	124.3(3)	Ti8—O37—Ti6	99.0(3)
Ti6—O3—Eu3	122.2(3)	Ti6—O3—Ti8	97.7(3)
Ti8—O3—Eu3	124.9(3)		

Table S23. Selected bond distances (\AA) of 6.

Atom-Atom	Length/ \AA	Atom-Atom	Length/ \AA
Eu1—O52	2.424(4)	Eu1—O13	2.402(4)
Eu1—O2	2.396(4)	Eu1—O17	2.409(4)
Eu1—N4	2.584(4)	Eu1—N8	2.364(3)
Eu1—O47	2.364(3)	Eu1—O25	2.336(3)
Eu3—O1	2.373(3)	Eu3—O8	2.329(3)
Eu3—O32	2.410(4)	Eu3—O39	2.408(4)
Eu3—O41	2.421(4)	Eu3—O21	2.401(4)
Eu3—N12	2.555(5)	Eu3—N9	2.583(5)
Ti1—O1	1.905(4)	Ti1—O4	2.063(3)
Ti1—O12	1.809(4)	Ti1—O26	2.102(4)
Ti1—O42	2.030(4)	Ti1—O25	1.888(3)
Ti2—O8	1.870(4)	Ti2—O12	1.870(4)
Ti2—O18	2.105(4)	Ti2—O22	2.011(4)
Ti2—O43	2.011(4)	Ti2—O47	1.919(3)
Ti7—O8	1.889(4)	Ti7—O19	2.110(4)
Ti7—O5	1.801(4)	Ti7—O11	2.012(4)
Ti7—O47	1.912(4)	Ti7—O51	2.061(3)
Ti8—O1	1.921(3)	Ti8—O20	2.013(3)
Ti8—O5	2.013(3)	Ti8—O23	2.028(4)
Ti8—O3	2.116(4)	Ti8—O25	1.870(4)

Table S24. Selected bond angles ($^{\circ}$) of **6**.

Atom-Atom-Atom	angles / $^{\circ}$	Atom-Atom-Atom	angles / $^{\circ}$
Ti1—O1—Eu3	121.81(18)	Ti1—O1—Ti8	96.18(15)
Ti8—O1—Eu3	124.63(17)	Ti2—O8—Eu3	123.31(17)
Ti2—O8—Ti7	98.90(16)	Ti7—O8—Eu3	125.47(19)
Ti1—O12—Ti2	142.4(2)	Ti2—O47—Eu1	125.41(17)
Ti7—O47—Eu1	121.62(17)	Ti7—O47—Ti2	96.38(15)
Ti1—O25—Eu1	126.08(19)	Ti8—O25—Eu1	126.08(19)
Ti8—O25—Ti1	98.56(16)		

Reference

- [1] (a) P. Hayoz and A. v. Zelewsky, *Tetrahedron Lett.*, 1992, **33**, 5165-5168. (b) P. Hayoz, A. V. Zelewsky and H. Stoeckli-Evans, *J. Am. Chem. Soc.*, 1993, **115**, 5111-5114. (c) X.-L. Li, Y. Zheng, J.-L. Zuo, Y. Song and X.-Z. You, *Polyhedron*, 2007, **26**, 5257-5262. (d) K. D. Oyler, F. J. Coughlin and S. Bernhard, *J. Am. Chem. Soc.*, 2007, **129**, 210-217.
- [2] J. L. Lunkley, D. Shirotani, K. Yamanari, S. Kaizaki and G. Muller, *J. Am. Chem. Soc.*, 2008, **130**, 13814-13815.
- [3] Y. Kitagawa, S. Wada, M. D. J. Islam, K. Saita, M. Gon, K. Fushimi, K. Tanaka, S. Maeda and Y. Hasegawa, *Commun. Chem.*, 2020, **3**, 119–123.
- [4] L. Arrico, C. Benetti and L. D. Bari, *ChemPhotoChem*, 2021, **5**, 815-821.
- [5] M. Górecki, L. Carpita, L. Arrico, F. Zinna and L. D. Bari, *Dalton Trans.*, 2018, **47**, 7166-7177.
- [6] M. Deng, N. F. M. Mukthar, N. D. Schley and G. I. Ung, *Angew. Chem.*, 2020, **59**, 1228-1231.
- [7] N. Hellou, M. Srebro-Hooper, L. Favereau, F. Zinna, E. Caytan, L. c. Toupet, V. Dorcet, M. Jean, N. Vanthuyne, J. A. Gareth Williams, L. D. Bari, J. Autschbach and J. Crassous, *Angew. Chem.*, 2017, **56**, 8236-8239.
- [8] J.-R. J. nez, B. Doistau, C. M. Cruz, C. Besnard, J. M. Cuerva, A. G. Campaña and C. Piguet, *J. Am. Chem. Soc.*, 2019, **141**, 13244-13252.
- [9] G. Park, H. Kim, H. Yang, K. R. Park, I. Song, J. H. Oh, C. Kim and Y. You, *Chem. Sci.*, 2019, **10**, 1294-1301.

- [10] Z. Han, X.-L. Zhao, P. Peng, S. Li, C. Zhang, M. Cao, K. Li, Z.-Y. Wang and S.-Q. Zang, *Nano Res.*, 2020, **13**, 3248-3252.
- [11] X.-Y. Wang, J. Zhang, J. Yin, S.-H. Liu and B.-Z. Tang, *Mater. Chem. Front.*, 2021, **5**, 368-374.
- [12] Z. Han, X.-Y. Dong, P. Luo, S. Li, Z.-Y. Wang, S.-Q. Zang and T. C. W. Mak, *Sci. Adv.*, 2020, **6**, eaay0107-eaay0114.
- [13] M.-M. Zhang, X.-Y. Dong, Z.-Y. Wang, X.-M. Luo, J.-H. Huang, S.-Q. Zang and T. C. W. Mak, *J. Am. Chem. Soc.*, 2021, **143**, 6048-6053.
- [14] M.-M. Zhang, X.-Y. Dong, Z.-Y. Wang, H.-Y. Li, Shi-Jun Li, X. Zhao and S.-Q. Zang, *Angew. Chem.*, 2020, **59**, 10052-10058.
- [15] Y.-J. Kong, Z.-P. Yan, S. Li, H.-F. Su, K. Li, Y.-X. Zheng and S.-Q. Zang, *Angew. Chem.*, 2020, **59**, 5336-5340.
- [16] S. Wada, Y. Kitagawa, T. Nakanishi, K. Fushimi, Y. Morisaki, K. Fujita, K. Konishi, K. Tanaka, Y. Chujo and Y. Hasegawa, *NPG Asia Mater.*, 2016, **8**, e251.
- [17] Y. Hasegawa, Y. Miura, Y. Kitagawa, S. Wada, T. Nakanishi, K. Fushimi, T. Seki, H. Ito, T. Iwasa, T. Taketsugu, M. Gon, K. Tanaka, Y. Chujo, S. Hattori, M. Karasawae and K. Ishii, *Chem. Comm.*, 2018, **54**, 10695-10697.
- [18] M. Zeng, A. Ren, W.-B. Wu, Y.-S. Zhao, C.-L. Zhan and J.-N. Yao, *Chem. Sci.*, 2020, **11**, 9154-9161.
- [19] T.-H. Zhao, J.-L. Han, X. Jin, Y. Liu, M.-H. Liu and P.-F. Duan, *Angew. Chem.*, 2019, **58**, 4978-4982.
- [20] H.-R. Fu, N. Wang, X.-X. Wu, F.-F. Li, Y. Zhao, L.-F. Ma and M. Du, *Adv. Optical Mater.*, 2020, **8**, 2000330.
- [21] P. Leo, G. Orcajo, J. A. Garcí'a, A. M. Ortun'o, J. M. Cuerva, D. Briones, G. Calleja, A. Rodrí'guez-Die'guez, b. Raul Sanz, J. Cepeda and F. Martí'nez, *J. Mater. Chem. C*, 2021, **9**, 5544-5553.
- [22] C.-T. Yeung, K.-H. Yim, H.-Y. Wong, R. Pal, W.-S. Lo, S.-C. Yan, M. Y.-M. Wong, D. Yufit, D. E. Smiles, L. J. McCormick, S. J. Teat, D. K. Shuh, W.-T. Wong and G.-L. Law, *Nat. Commun.*, 2017, **8**, 1128.
- [23] Y.-Y. Zhou, H.-F. Li, T.-Y. Zhu, T. Gao and P.-F. Yan, *J. Am. Chem. Soc.*, 2019, **141**, 19634-19643.
- [24] Y.-L. Ding, C.-S. Shen, F. Gan, J.-H. Wang, G.-L. Zhang, L.-L. Li, M.-H. Shu, B.-S. Zhu, J. Crassous and H.-B. Qiu, *Chin. Chem. Lett.*, 2021, **32**, 3988-3992.
- [25] C.-J. Li, Yuan-Yuan Liu, Y.-P. Wang, J. Guo and M. Pan, *Sci. Sin. Chim.*, 2020, **50**, 687-694.
- [26] J. Kumar, B. Marydasan, T. Nakashima, T. Kawaia and J. Yuasa, *Chem. Comm.*, 2016, **52**, 9885-9888.
- [27] Z.-W. Yao, Y.-Y. Zhou, T. Gao, P.-F. Yan and H.-F. Li, *RSC Adv.*, 2021, **11**, 10524-10531.
- [28] Y. B. Tan, Y. Okayasu, S. Katao, Y. Nishikawa, F. Asanoma, M. Yamada, J. Yuasa and T. Kawai, *J. Am. Chem. Soc.*, 2020, **142**, 17653-17661.

- [29] T. Ono, K. Ishihama, A. Taema, T. Harada, K. Furusho, M. Hasegawa, M. A. Yuki Nojima and Y. Hisaeda, *Angew. Chem.*, 2021, **60**, 2614-2618.
- [30] H. Ito, H. Sakai, Y. Okayasu, J. Yuasa, T. Mori and T. Hasobe, *Chem. Eur. J.*, 2018, **24**, 16889-16894.
- [31] N. Wang, J.-J. Zhao, Q. Xu, P.-Y. Xing, S.-Y. Feng, X.-D. Xu and H.-B. Yang, *J. Mater. Chem. C*, 2022, **10**, 13860-13870.
- [32] G.-F. Huo, Q. Tu, Y.-X. Hu, B. Jiang, Q.-F. Zhou, Y.-F. Niu, X.-L. Zhao, H.-M. Ding, J. Wen, G.-Q. Yin, X.-L. Shi and L. Xu, *Sci. China Mater.*, 2021, **65**, 469-476.
- [33] Q.-Y. Zhu, L.-P. Zhou, L.-X. Cai, X.-Z. Li, J. Zhou and Q.-F. Sun, *Chem. Comm.*, 2020, **56**, 2861-2864.
- [34] L. Arrico, L. D. Bari and F. Zinna, *Chem. Eur. J.*, 2021, **27**, 2920-2934.